An idea to treat the dendritic morphology in mixed columnar–equiaxed solidification

M. Wu* and A. Ludwig

To treat mixed columnar–equiaxed solidification with dendritic morphology, five phase regions have been distinguished: extradendritic melt, interdendritic melt and solid dendrites in equiaxed grains, interdendritic melt and solid dendrites in columnar arrays of dendrites. These five phases are quantified by their volume fractions, and characterized by different volume-averaged solute concentrations. The equiaxed grains and columnar dendrites are confined by their envelopes, whose shapes are described by morphological parameters. The evolution of the envelopes is derived based on recent growth theories: the growth of primary columnar dendrite tips by the Kurz–Giovanola–Trivedi (KGT) model, the growth of secondary dendrite tips in radial direction of columnar trunk and the equiaxed dendrite tips by the Lipton–Glicksman–Kurz (LGK) model. The solidification of the interdendritic melt is governed by diffusion in the interdendritic melt region. Preliminary modelling results on a benchmark casting (Al–4·7wt-% Cu) show the potentials of the model.

Keywords: Mixed columnar–equiaxed solidification, Dendritic morphology, Columnar-to-equiaxed transition, Macrosegregation

Introduction

Wang and Beckermann (WB)[1,2] have outlined a general multiphase approach for dealing with the dendritic morphology in equiaxed or columnar solidification. With the idea similar to the Rappaz and Thevoz model (RT),[3,4] they defined a grain envelope to separate the extra dendritic melt from the interdendritic melt. Because columnar dendrites and equiaxed grains have different morphologies, different formulations and morphological parameters must be considered. The current work is to implement the above idea into a previously-developed 3-phase mixed columnar-equiaxed solidification model by the authors.[5,6] The main features of the previous 3-phase mixed columnar–equiaxed solidification model is to consider melt convection, grain sedimentation, columnar tip front tracking, interaction between equiaxed grains and columnar dendrites, columnar-to-equiaxed transition, etc. The current paper gives only a general description of model, and presents preliminary modelling results for an Al–4·7Cu benchmark casting.

Definition of phase regions and morphology assumptions

The volume fraction of the above mentioned five phases are defined as follows: extradendritic melt, f_ℓ, interdendritic melt in the equiaxed grain, f_ℓ^{e}, and solid dendrite in the equiaxed grain, $f_{\mathrm{s}}^{\mathrm{e}}$, interdendritic melt in the columnar trunk, f_ℓ^{c}, and solid dendrite in the columnar trunk, $f_{\mathrm{s}}^{\mathrm{c}}$. The interdendritic melt and solid dendrite in the equiaxed grain combine to form a 'hydrodynamic' e-phase, moving with an average velocity, while the interdendritic melt and solid dendrite in the columnar trunk combine to form another 'hydrodynamic' c-phase, moving with a predefined velocity. The interdendritic melt is separated from the extra dendritic melt by a grain boundary, i.e. the grain envelope. The extra dendritic melt is regarded as a third 'hydrodynamic' phase, ℓ-phase, having a velocity . The transport of mass, species and energy of each phase region is calculated based on the velocity of the corresponding 'hydrodynamic' phase. The columnar tip front divides the whole physical domain into two: in front of the columnar tip front, the number of 'hydrodynamic' phases is 2, i.e. ℓ- and e-phases, thus there are only 3 phases involved. Behind the columnar tip front, all the 3 'hydrodynamic' phases (ℓ-, e- and c-phases) and all the 5 phase regions ($f_\ell, f_\ell^{\mathrm{e}}, f_{\mathrm{s}}^{\mathrm{e}}, f_\ell^{\mathrm{c}}, f_{\mathrm{s}}^{\mathrm{c}}$) might be involved. The columnar tip front is explicitly tracked.[5,6]

An improved model for the equiaxed dendritic solidification was presented previously.[7] As shown in Fig. 1, the grain envelope (dashed line) is defined as a fictitious surface connecting the primary and secondary dendrite tips. The interdendritic melt has an averaged concentration c_ℓ^{e}, while the extra dendritic melt has a concentration c_ℓ. When the grain envelope grows, both the species transfer due to the growth of the envelope and the species diffusive flux cross the envelope are considered.[7] Solidification occurs only at the solid–liquid interface, i.e. the interface between the interdendritic melt and solid dendrites, where a thermodynamic equilibrium condition applies. The interdendritic melt

Department of Metallurgy, University of Leoben, A-8700 Leoben, Austria, Phone: +43 3842 4022223, Fax: +43 3842 4022202

*Corresponding author, email menghuai.wu@mu-leoben.at

Received 17 June 2008; accepted 12 September 2008
DOI 10.1179/136404609X368082

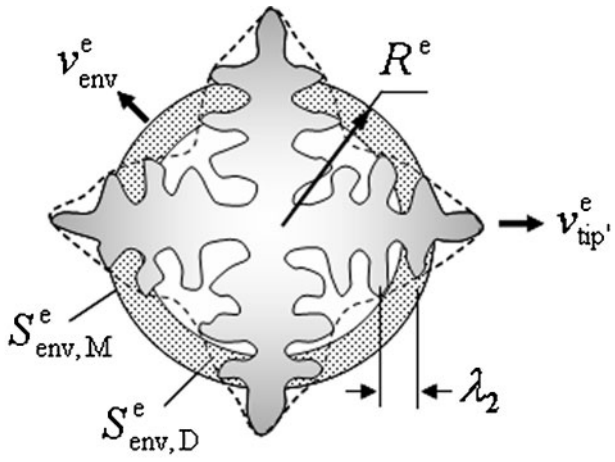

1 The shape of the equiaxed dendritic grain is simplified as a sphere with the equivalent volume of the fictitious grain envelope connecting the primary and secondary dendrite tips

and solid adjacent to the solid-liquid interface has the equilibrium concentrations c^*_ℓ and c^*_s, dictated by the local temperature according to thermodynamics. It is the concentration difference $(c^*_\ell - c^e_\ell)$ that serves as driving force for the solidification of the interdendritic melt. Latent heat is released, and solute partitioning $(k = c^*_s/c^*_\ell)$ occurs at the solid–liquid interface.

The local growth velocity of the fictitious grain envelope (dashed line, Fig. 1) is unknown. What is known from the classical tip growth kinetics is the primary tip growth velocity $v^e_{tip'}$, e.g. by the LGK model.[8] Therefore, we further simplify the shape of the equiaxed dendritic grain as an 'equivalent sphere', with its volume equivalent to the volume enclosed in the fictitious grain envelope. By defining a shape factor Φ^e_{env},[7] we can obtain the growth velocity of the equivalent sphere from the primary tip growth velocity:

$$v^e_{env,\,S} = \Phi^e_{env} \cdot v^e_{tip'} \tag{1}$$

In order to calculate the species diffusive flux at the envelope between the interdendritic and extradendritic melts, however, the real surface area of the envelope $S^e_{env,D}$ is required. This area $S^e_{env,D}$ is actually correlated to the surface area of the equivalent sphere $S^e_{env,S}$ by another factor Φ^e_{sph}, which is called sphericity,

$$S^e_{env,D} = S^e_{env,S}/\Phi^e_{sph} \tag{2}$$

Both Φ^e_{env} and Φ^e_{sph} are two morphological parameters, dependent purely on the shape of the grain envelope. If the shape of the grain envelope is preserved and constant, then they can be determined previously. For example, in the RT model,[3,4] an ideal sphere envelope connecting the primary dendrite tips is assumed, both Φ^e_{env} and Φ^e_{sph} are equal to one. For an octahedral envelope considered by Nielsen *et al.*,[9] Φ^e_{env} is $1/\sqrt[3]{\pi}$ and Φ^e_{sph} is $\sqrt[3]{\pi}/\sqrt{3}$. For a general case (Fig. 1), both morphological parameters might be smaller than the values mentioned above. By using the above two morphological parameters the nature of the arbitrary shape of the grain envelope with a simplified equivalent sphere can be approaximated.

For the columnar growth, the dendrite trunk is enclosed in a fictitious dendrite envelope, as shown in Fig. 2 (dash line). Near the primary dendrite tip, it encloses the primary dendrite tip and secondary dendrites, while in the trunk region (away from the primary dendrite tip) it encloses the secondary and tertiary dendrites. The longitudinal section of the envelope near the primary dendrite tip is parabolic, while the cross section of dendrite trunk can be approximated by a quadrate or cloverleaf. Therefore, the consideration for the region near primary dendrite tip is different from the one for the columnar dendrite trunk region.

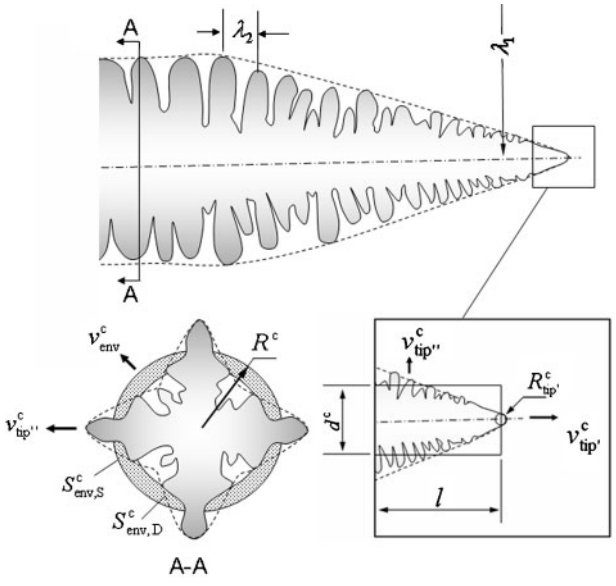

2 The shape of the columnar dendrite trunk is simplified as a step-wise cylinder with the cross section area equivalent to the fictitious tree-trunk envelope connecting the secondary and tertiary dendrites. The parabolic shape of the columnar envelope near the primary dendrite tip is also simplified as an equivalent cylinder with an averaged diameter and explicitly-tracked length

For the columnar trunks, the dendrite envelope is further simplified as a step-wise growing cylinder with the cross section area equivalent to the enclosed area of the dendrite envelope. The growth speed of the cylinder in radial direction can be derived from the growth velocity of the secondary dendrite tip $v^c_{tip''}$,

$$v^c_{env,\,C} = \Phi^c_{env} \cdot v^c_{tip''} \tag{3}$$

where Φ^c_{env} is a shape factor. The diffusion area of the columnar envelope $S^c_{env,D}$ is calculated based on the surface area of the equivalent cylinder $S^c_{env,C}$ by considering a circularity Φ^c_{circ},

$$S^c_{env,D} = S^c_{env,C}/\Phi^c_{circ} \tag{4}$$

Both Φ^c_{env} and Φ^c_{circ} are morphological parameters ($\leqslant 1$). When the envelope of columnar trunk (dashed line in Fig. 2) is identical to an ideal circle (cross section of a cylinder), they are equal to one. If cross section of the dendrite trunk envelope is close to a quadrate, then $\Phi^c_{env} = \sqrt{2/\pi}$, $\Phi^c_{circ} = \sqrt{\pi}/2$. For any other complicated envelopes, both morphological parameters are smaller than the values mentioned above. With these morphological parameters, any arbitrary cross-section of the dendrite trunk envelope can be approximately described with an equivalent circle.

In the columnar dendrite tip region, the parabolic envelope is approximated as an equivalent cylinder with an averaged diameter d^c and length l (Fig. 2). The length of the cylinder is tracked with a method described previously.[10] With the corresponding shape factor and circularity, the dendritic morphology of the primary dendrite tip region is modelled.

Growth kinetics

Equiaxed growth

Two situations are distinguished:[7] globular growth and dendritic growth. For the globular growth, solute partitioning occurs at the solid-liquid phase boundary (identical to the grain envelope). The growth of the grain is governed by diffusion around the spherical grain, and its growth velocity v^e_{glob} can be obtained analytically

$$v^e_{glob} = \frac{D_\ell}{R^e} \cdot \Omega, \tag{5}$$

where Ω is the constitutional undercooling $(c^*_\ell - c_\ell)/(c^*_\ell - c^*_s)$. For the dendritic growth, the growth velocity of the dendrite tips $v^e_{tip'}$ can be determined by the LGK model.[8] With equation (1) the growth velocity of the equivalent sphere of dendritic grain is obtained $v^e_{env,\,S}$. The globular-to-dendritic transition (GDT) is determined by comparing the two growth velocities, v^e_{glob} and $v^e_{env,\,S}$.

$$v^e_{env} = \max(v^e_{glob}, \quad v^e_{env,\,S}) \tag{6}$$

The growth surface area concentration $S^e_{env,\,M}$ of the equivalent spheres is calculated

$$S^e_{env,\,S} = \Phi^e_{Imp} \cdot (36\pi \cdot n)^{\frac{1}{3}} \cdot f_e^{\frac{2}{3}}, \tag{7}$$

where n is number density of the grains, and Φ^e_{Imp} is an impingement factor for the growing grains. With the v^e_{env} and $S^e_{env,\,S}$, the volume averaged mass transfer rate from the ℓ-phase to the e-phase can be calculated.

Columnar growth

Again, two situations are to be distinguished: cellular growth (non-dendritic) and dendritic growth. For the cellular growth, its radial growth velocity v^c_{cell} is governed by the diffusion,

$$v^c_{cell} = \frac{D_\ell}{R^c} \cdot \Omega \cdot \ln^{-1}\left(\frac{\lambda_1}{\sqrt{3}R^c}\right) \tag{8}$$

Here a staggered arrangement of the cellular trunks is assumed. The actual cellular diameter is $2R^c$, and the far field reference diameter is $2\lambda_1/\sqrt{3}$. For the dendritic growth, the radial growth velocity of the secondary dendrite tip $v^c_{tip''}$ is determined by the LGK model.[8] With Eq.(3) the growth velocity of the equivalent cylinder of the columnar dendrite trunk is obtained $v^c_{env,\,C}$. The cellular-to-dendritic transition (CDT) is determined by comparing the above two growth velocities, v^c_{cell} and $v^c_{env,C}$

$$v^c_{env} = \max(v^c_{cell}, \quad v^c_{env,\,C}) \tag{9}$$

The growth surface area concentration $S^c_{env,\,C}$ of the equivalent cylinder is calculated

$$S^c_{env,\,C} = \Phi^c_{Imp} \cdot \frac{2\pi R^c}{\lambda_1^2} \tag{10}$$

where Φ^c_{Imp} is an impingement factor for the growing columnar trunks. With v^c_{env} and $S^c_{env,\,C}$, the volume averaged mass transfer rate from the ℓ-phase to the c-phase in the volume elements, which contain the fully over-grown columnar trunks, can be calculated.

In the volume elements which contain columnar tips, some special considerations must be made. For the growth of the equivalent cylindrical envelope in the radial direction, the same idea of Eq. (8)–(9) is used to get v^c_{env}, but the length of the columnar trunks l which is contained in the volume element and the corresponding diameter, $d^c/2$, must be tracked explicitly.[10] Additionally, the contribution of the growth of the primary tips themselves ($v^c_{tip'} \cdot \pi R^c_{tip'} 2$) to the total volume averaged mass transfer in the considered volume element must also be taken into account. The tip radius $R^c_{tip'}$ is estimated according to Kurz and Fisher,[11] and the primary tip growth velocity $v^c_{tip'}$ is according to KGT model.[12]

The solidification of the interdendritic melt is treated in the same way for both equiaxed and columnar growth and is described elsewhere.[7]

Modelling example

The solidification of an Al-4·7wt-%Cu cylindrical casting is simulated. Mould filling is ignored. The casting starts to solidify from an initial temperature of 922 K. A constant heat transfer coefficient (500 W m^2 K^{-1}) between casting and mould (290 K) and a constant heat transfer coefficient (100 W m^2 K^{-1}) between casting and air (290 K) at the top are applied. The thermophysical and dynamical data used are given elsewhere,[7,14] and some other modelling parameters are listed in Table 1.

The final simulation results are shown in Fig. 3. The most important information, such as the macrostructure distribution with distinguished columnar and equiaxed zones separated by the CET line, the rest of eutectic which are distributed in the interdendritic region f^{intern}_{Eu} and in the extra grain region f^{extra}_{Eu}, and the final

Table 1 Parameters used for the simulation

Nucleation parameters:
$n_{max} = 5 \times 10^{10}$ m^{-3}
$\Delta T_N = 10$ K
$\Delta T_\sigma = 0{\cdot}5$ K
Growth kinetics parameters in KGT model:[12,13]
$v^c_{tip'} = k_1 \cdot \Delta T^2 + k_2 \cdot \Delta T^3$
where ΔT is the undercooling and k_1 and k_2 are
$k_1 = 1{\cdot}16633 \times 10^{-4} \cdot (100 \cdot c_\ell)^{-1.24319}$
$k_2 = 5{\cdot}39996 \times 10^{-4} \cdot (100 \cdot c_\ell)^{-2.13518}$

Morphological parameters:
$\Phi^e_{env} = 0{\cdot}6827$;
$\Phi^e_{sph} = 0{\cdot}283$;
$\Phi^c_{env} = 0{\cdot}7979$;
$\Phi^e_{circ} = 0{\cdot}295$;
$\lambda_1 = 500$ μm;
$\lambda_2 = 10$ μm.

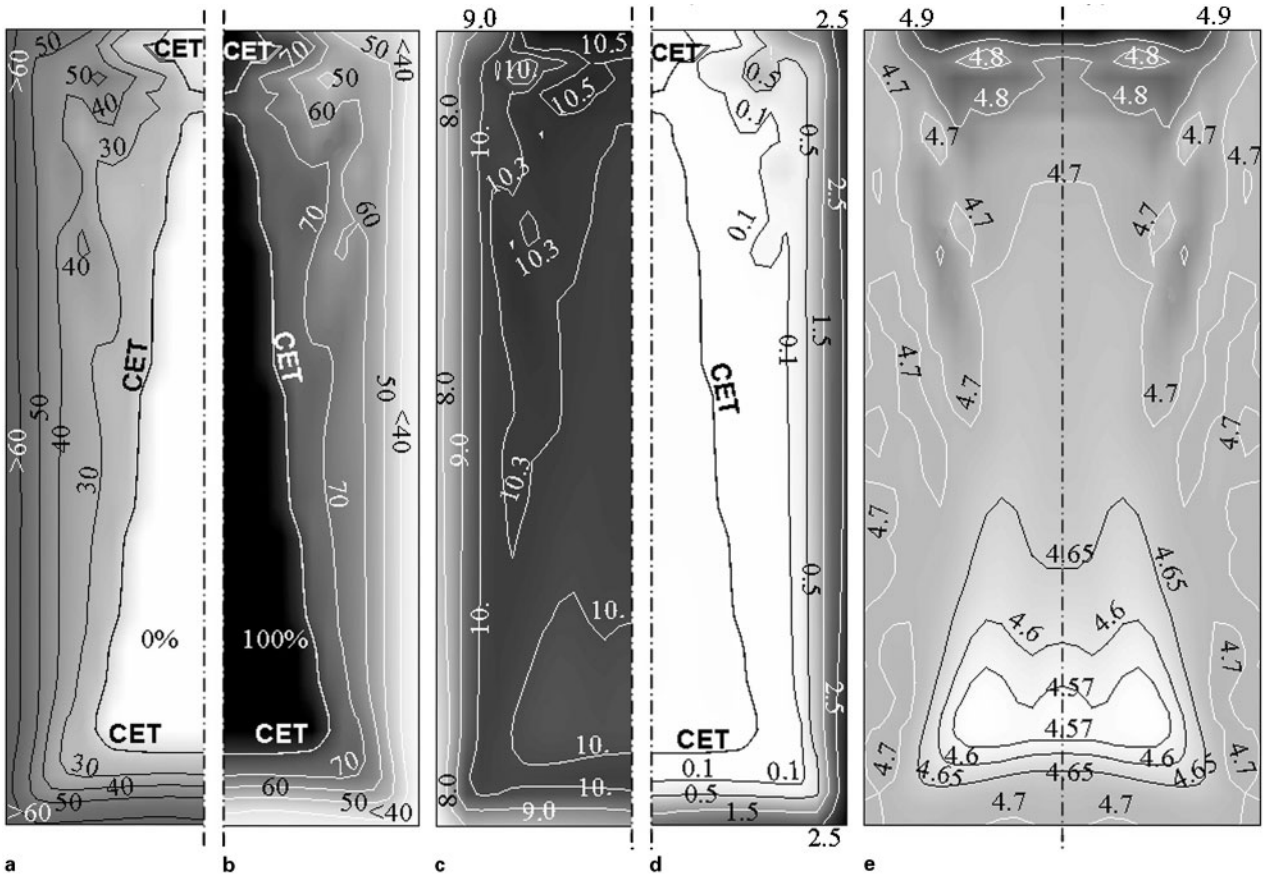

3 Predicted as-cast macrostructure and macrosegregation. The quantities are shown with both isolines and grey scale (dark for highest, light for lowest). Columnar-to-equiaxed transition is indicated with CET line. a) volume percent distribution of columnar dendrite trunks; b) volume percent distribution of equiaxed grains; c) interdendritic eutectic including those in equiaxed grains and in columnar trunks; d) extradendritic eutectic; e) macrosegregation distribution in mass percent

macrosegregation c_{mix} pattern, etc. can be obtained. These macrostructure information and concentration distribution pattern are outcome of the global heat transfer, morphology evolution including GDT and CDT, competition between the progress of grain envelope and interdendritic melt solidification, melt flow and grain sedimentation. Equiaxed grains nucleate and grow from corner, surface and bulk regions, while columnar trunks grow directly from the mould walls. Both grow competitively. The equiaxed grains sink because of their higher density, and they finally reach the bottom region and settle there. While some of the equiaxed grains sink along the columnar tip front, some of them are captured by the growing columnar tips. This entrapment phenomenon is more evidently observed in the bottom region when large amounts of equiaxed grains settle there. This dynamic phenomenon contributes greatly to the final solidification microstructure.

Summary

A volume average model is proposed to consider the dendritic morphology in the mixed columnar-equiaxed solidification. 5 phase regions, and their evolution and transport phenomena are considered. The preliminary modelling results on an Al-4·7wt-% Cu benchmark casting have shown the potentials of the model: the evolution and transport of the phase regions, the formation of the macrostructure (i.e. the distinguished equiaxed zone from the mixed columnar-equiaxed zone separated by the CET line), the formation of the primary phase and eutectics, and the macrosegregation caused by melt convection and grain sedimentation. However, the model is still subject to further refinements and evaluations.

References

1. C. Y. Wang and C. Beckermann: *Metall. Mater. Trans.*, 1993, **24A**, 2787–2802.
2. C. Y. Wang and C. Beckermann: *Metall. Mater. Trans.*, 1996, **27A**, 2754–2764.
3. M. Rappaz and Ph. Thévoz: *Acta Metall.*, 1987, **35**, 1478–1497.
4. M. Rappaz and Ph. Thévoz: *Acta Metall.*, 1987, **35**, 2929–2933.
5. A. Ludwig and M. Wu: *Mater. Sci. Eng. A*, 2005, **413–414**, 109–114.
6. M. Wu and A. Ludwig: *Metall. Mater. Trans.*, 2006, **37A**, 1613–1631.
7. M. Wu and A. Ludwig: Proc. 5th Decennial Intern. Conf. on Solidification Processing, July 23–25, 2007, Sheffield, UK. Ed. H. Jones., University of Sheffield, 130–135.
8. J. Lipton, M. E. Glicksman and W. Kurz: *Mater. Sci. Eng.*, 1984, 65, 57–63.
9. Ø. Nielsen, B. Appolaire, H. Combeau and A. Mo: *Metall. Mater. Trans.*, 2001, **32A**, 2049–2060.
10. M. Wu and A. Ludwig: *Metall. Mater. Trans.*, 2007, **38A**, 1465–1475.
11. W. Kurz and D. J. Fisher: 'Fundamentals of Solidification', Trans Tech Publications, Aedemannsdorf, Switzerland, 1989.
12. W. Kurz, B. Giovanola and R. Trivedi: *Acta Metall.*, 1986, **34**, 823–834.
13. S. Y. Lee, S. M. Lee and C. P. Hong: *ISIJ Int.*, 2000, **40**, 48–57.
14. M. Wu, A. Ludwig and J. Luo: *Mater. Sci. Forum*, 2005, **475–479**, 2725–2730.